8

Geomorphic Landforms and Tectonism Along the Eastern Margin of the Okavango Rift Zone, North Western Botswana as Deduced From Geophysical Data in the Area

E.M. Shemang and L.N. Molwalefhe
Department of Geology, University of Botswana, Gaborone
Botswana

1. Introduction

The location, orientation, and evolution of normal faults that form during continental rifting exert a strong influence on the development of regional features (geomorphology, drainage patterns, basin location, stratigraphy, location of magmatism, and if the process of continental rifting is successful, the geometry of the passive margin) of the rift. Understanding the factors which control the growth and propagation of normal faults at the earliest stages of continental rifting will lead to a better overall understanding of the processes which control the development of continental rifts – an essential component of the plate tectonics paradigm.

There are only a few examples of young continental rifts which are suitable for the investigation of the process of border fault development and evolution. The Okavango Rift Zone (ORZ), in northwestern part of Botswana (Fig. 1) is one example of a zone of incipient continental rifting (Scholz et al., 1976; Modisi et al., 2000). Recent studies suggest that faults associated with this rift are still in a juvenile stage (Kinabo et al., 2007), therefore the ORZ provides us with a unique opportunity to investigate the earliest developmental stages of continental rifts such as fault growth and propagation. In areas where the faults are mostly buried beneath large accumulations of sediment, have subdued surface relief, and or where access and travel is limited, as is the case in the ORZ (Kinabo et al., 2007; Modisi et al., 2000), it is difficult to accomplish structural mapping of such areas. For these areas, important structural information regarding rift processes can be obtained from magnetic data (Modisi et al. 2000; Grauch, 2000). Other studies including Chen and Lee (1982); Kervyn et al., (2006) have also shown the utility of Digital Elevation Models (DEM) to map rift fault morphology. In this study, high resolution aeromagnetic (HRAM) data (which provide information about the faulting within the basement) has been used together with SRTM DEM data (which provide surface morphological expression of the faults) to provide a clear perspective of faults and fault patterns associated with ORZ. The information from these sources (HRAM and SRTM DEM) is used to examine stages of fault growth, linkage, and propagation within the ORZ.

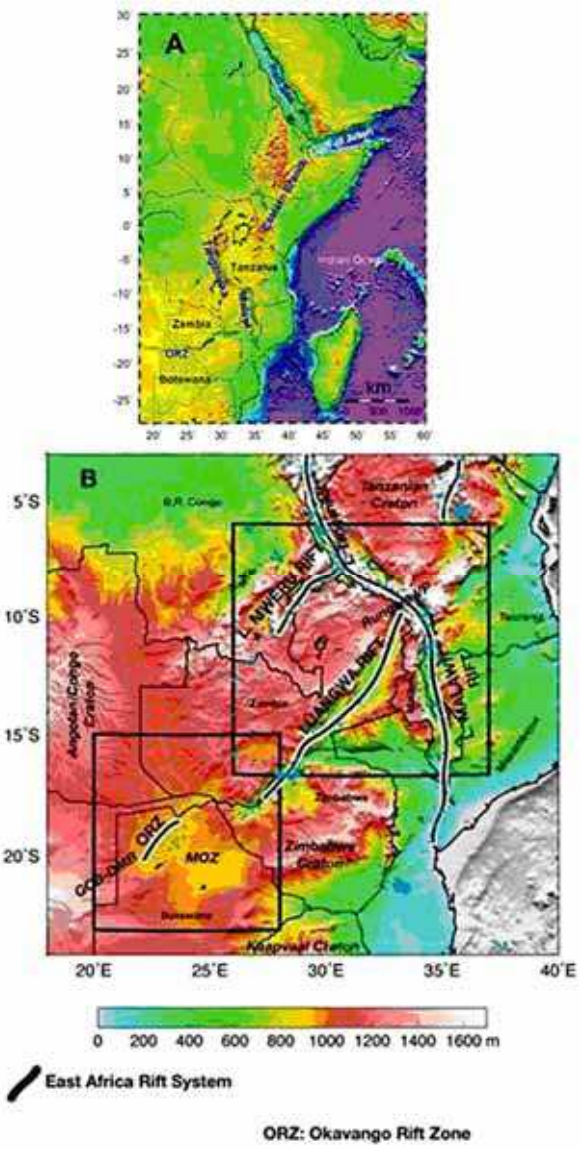

Fig. 1. Location of the Okavango Rift Zone (B) in relation to (A) the East African Rift System (EARS): Note scale - scale is for (B) only

2. The Okavango Rift Zone

The Okavango Rift Zone (Figure 1) is an incipient continental rift located in the north-western part of Botswana. It occurs in an intercratonic zone between the Congo craton to the northwest and the Kalahari craton (consisting of the Zimbabwe and Kaapvaal cratons) to the

east-southeast (e.g., Kinabo et al., 2007; 2008). The development of the ORZ is thought to be taking place within a large structural depression known as the Makgadikgadi-Okavango-Zambezi basin (MOZ) and is characterized by northeasterly trending folds and faults of the Ghanzi-Chobe belt (Cooke, 1984).

The strike of the main bounding rift-related faults is 030 – 050° in the north and 060 – 070° in the south (Kinabo et al., 2007; 2008). The orientation of the faults on the surface is influenced by pre-existing faults and folds of the basement rocks (Modisi et al., 2000; Kinabo et al., 2007; 2008).

The MOZ basin comprised of both alluvial fan deposits and deeper palaeo-lake sediments in structural depressions or sub-basins (Gumbricht et al., 2001; Shaw and Nash 1998). This rift basin hosts the largest in-land alluvial fan on Earth, supporting the largest (~18 000 km^2) wetland in southern Africa (McCarthy et al., 1991). It is believed that this fan owes its origin to neotectonic activity related to the East African Rift system (Fairhead & Girdler, 1969; Scholz et al., 1976; McCarthy et al., 2001; Modisi, 2000; Modisi et al., 2000).

Initiation of current rifting processes in the ORZ are unknown; however, paleoenvironmental reconstruction from sediments collected in Lake Ngami suggests that feeder rivers promoted extensive flow beyond the Thamalakane and Kunyere faults circa and beyond into the Makgadikgadi pans (Shaw, 1995). Between 120 Ka and ~ 40 Ka, neotectonic activity resulted in uplift along the Zimbabwe-Kalahari axis and displacement along the northeast-southwest trending faults resulting in the impoundment of the proto-Okavango, Kwando, and the upper Zambezi rivers and the development of the proto-Makgadikgadi, Ngami, and Mababe sub-basins (Cooke 1984; Thomas and Shaw, 1991; Moore and Larkin, 2001) suggesting that rifting may have been initiated about 40 Ka.

3. Geological setting

Except for a few isolated outcrops, the rocks in the ORZ are largely buried underneath an extensive desert sand cover (Kalahari Sands). Pre-Okavango geologic units which include the marls, clays, gravels, eolian sands, calcrete, and silcrete define the 230-m-thick Cenozoic Kalahari beds; Carboniferous to Jurassic Karoo supracrustal sequences include sedimentary and volcanic rocks. A prominent geologic feature seen in the area is the west-northwest–trending Karoo dike swarm. Neoproterozoic siliciclastic and carbonate sequences compose the Ghanzi-Chobe Supergroup and lies to the south western edge of the ORZ while Mesoproterozoic metavolcanic rocks and related granitoids and gneisses are underlain by Paleoproterozoic basement (gneiss, granulite, granitoids). Proterozoic structures (fold axes, thrusts) trend northeast-southwest; transverse shear zones trend east-west and west-northwest (Modisi et al., 2000)

4. Data acquisition and processing

The data set includes high-resolution aeromagnetic data acquired in 1996 under the direction of the Department of Geological Survey, Botswana. The mean flight elevation was 80 m along north-south lines 250 m apart, with east-west tie lines 1.25 km apart. The International Geomagnetic Reference Field has been removed from the observed data. The data were gridded (i.e., with a grid cell size of 62.5 m) using minimum curvature technique (Briggs, 1974; Swain, 1976). Minimum curvature gridding is accomplished by fitting a

smoothest possible surface to data values. Vertical derivative filters were applied to the total field magnetic data in order to enhance shallow seated features of the rift and the basement. Depth to the top of the dikes was determined using Euler's homogeneity equation (Thompson, 1982), with depth errors of ±3 m. Three arc (SRTM-3, 90 m X-Y resolution data and ± 30 m root mean square error z accuracy) were used to produce a mosaic image of the study area.

5. Results

The most prominent features on the aeromagnetic maps are the west-northwest–trending late Karoo dykes (Fig. 2). This approximately 70-km-wide dike swarm extends from Zimbabwe in the east, through the study area in Botswana, into northeastern part of Namibia to the northwest (Reeves, 1972). The dykes are superimposed on northeasterly trending folds and faults of the Neoproterozoic Ghanzi- Chobe belt and are cut by younger faults (Fig. 2).

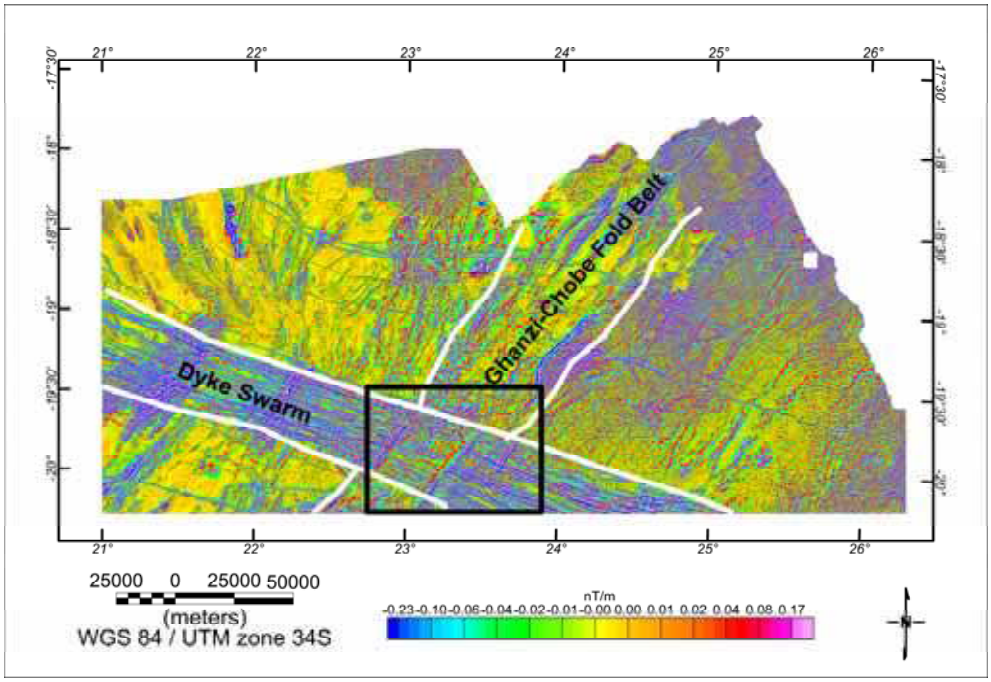

Fig. 2. First vertical derivative anomaly map of the Northern part of Botswana Including the Okavango Rift Zone. The box shows the selected area to detail investigation shown in Figure 3

In order to study the nature of faulting at the southeastern margin of the ORZ, an area was selected (see figure 2 for location of the selected area) for a more detailed analysis. First and second vertical derivative filters were applied to the total field magnetic data in the selected area, in order to enhance shallow seated features of the rift and the basement. The features

enhanced include basement structural features such as dikes, faults, fractures, and folds. Figure 3 is a map showing the results of a first vertical derivative of the total magnetic anomalies in the selected area. From this figure, four major northeast-trending faults are evident within this area: the Kunyere, Thamalakane, Phuti, and Nare faults (Fig. 3). These faults cut across as well as displace the dikes in the area. Three of them (Kunyere, Thamalakane and Phuti) are represented by fault scarps on the digital terrain map (Figures 4 and 5). Preexisting northeast-trending basement fabric controls the trend of these faults.

Three profiles were chosen across these faults (see Figure 6 for the location of the profiles) and the plots of these profiles are presented in Figure 7. The locations of the prominent faults mapped out in the area are indicated on the different profiles. Profile A, is located more to the south western part of the study area, while profile C is to the north east of the study area. From the figure, magnetic signature of the faults becomes more prominent as you move from north east to south west. This possibly suggests that magnetic sources are much closer to the surface in the south western section of the study area than in the north eastern portion. This could possibly indicate that fault throws in the north western part of the study area are smaller as compared to the north eastern sector.

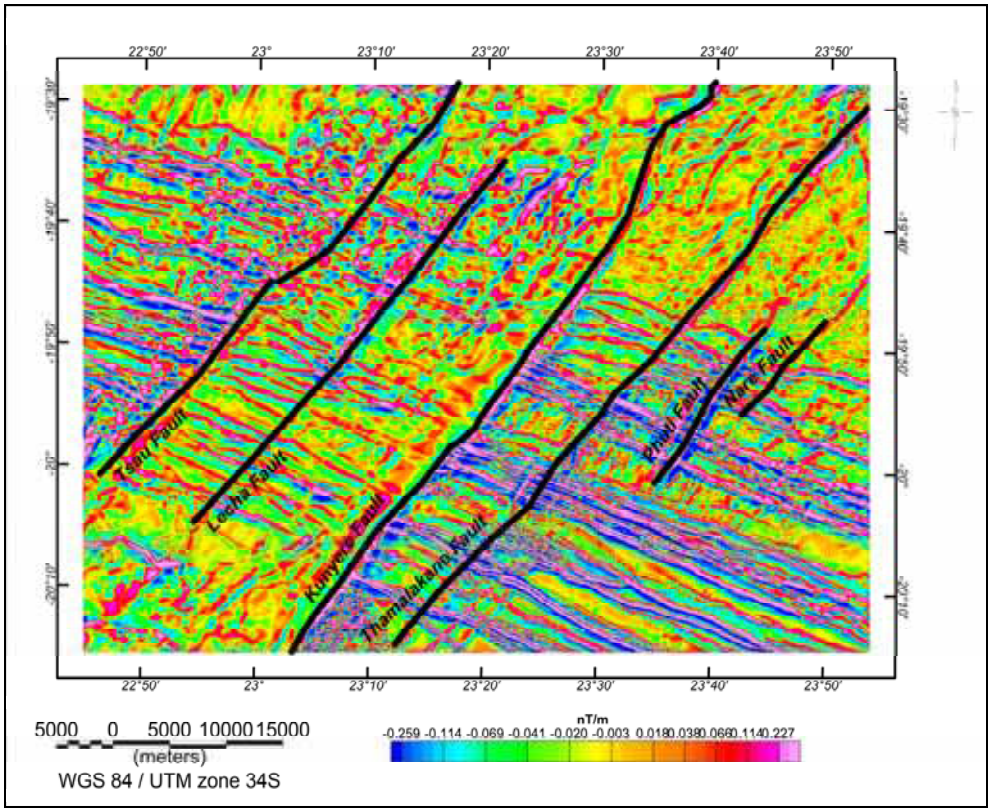

Fig. 3. First vertical derivative anomaly map of the study area

Depths to the top of magnetic sources were determined from 3-D Euler depth solutions. The 3-D Euler deconvolution technique uses the derivative of the signal in three dimensions (xyz) to estimate depth from an arbitrary surface to the top of a representative structure. The technique uses the Euler homogeneity equation which can be written in the form below

$$(x-x_0)\frac{\partial_T}{\partial_x}+(y-y_0)\frac{\partial_T}{\partial_y}+(z-z_0)\frac{\partial_T}{\partial_Z}=N(B-T)$$

Where (x_0, y_0, z_0) is the position of a magnetic source whose total field T is detected at (x, y, z) (Thompson, 1982). The total field has a regional value of B and N is the structural index. Parameters for the depth estimates included a structural index of 1 for dikes, which were used as displacement markers because of their pervasiveness in the area and their crosscutting relationship with the rift faults. Depth solutions with depth tolerance of greater than 5% were discarded. Figure 8 is a plot showing the results of the 3-D Euler deconvolution in the selected area of study.

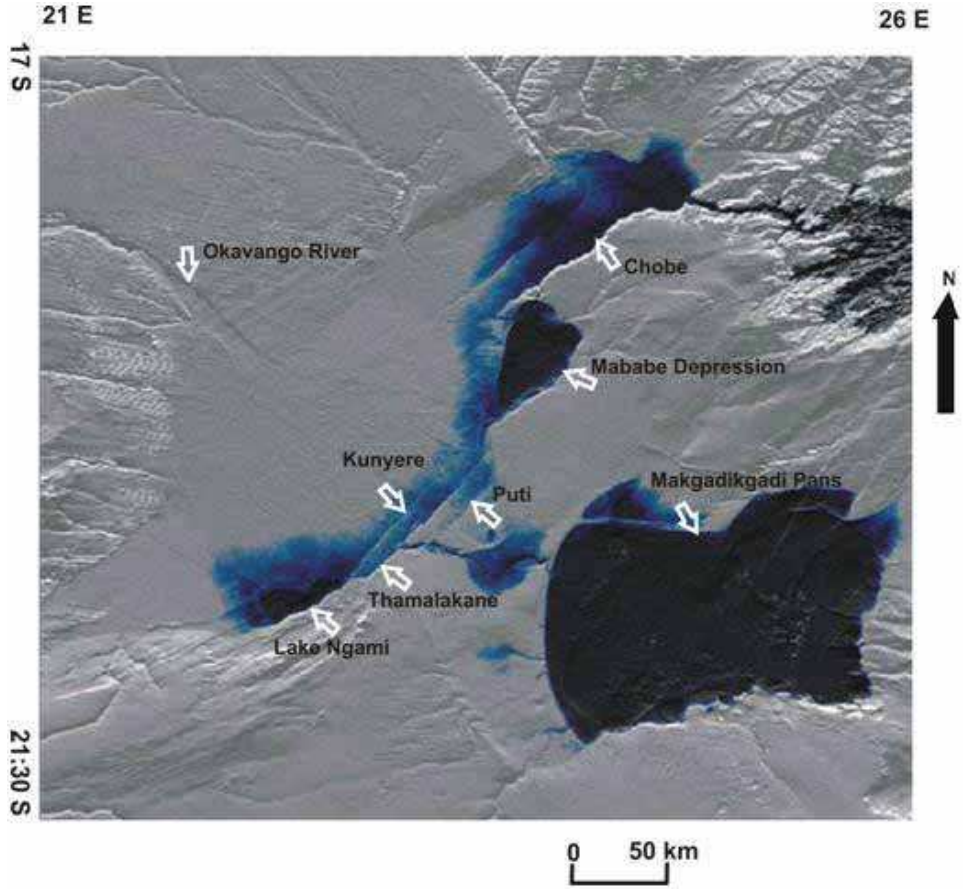

Fig. 4. Plot of SRTM for the ORZ area

Vertical throws across faults were estimated by taking the difference in depth between two segments of the dike displaced by faults (Fig. 7). Euler deconvolution results presented in Figure 7 were used to determine the vertical displacement along faults.

6. Discussion

6.1 Faulting in the area

Six major northeast-trending faults are evident in the study area; the Tsau, Lecha, Kunyere, Thamalakane, Phuti, and Nare faults (Figures 3 and 8). These faults displace the dykes and three of them (Kunyere, Thamalakane and Phuti) are represented by fault scarps on the digital terrain map (Fig 4 and 5). Preexisting northeast-trending basement fabric controls the trend of these faults. Depth estimates to the top of the dikes show a deepening of the pre-Kalahari surface toward the northeast (Fig. 8). To the south west of the Kunyere fault, average depths calculated are lower as compared to the northeast, where depths are generally more than 600m. From these results, dip-slip movements were inferred; blocks are downthrown to the west consistent with seismic reflection interpretations (Laletsang, 1995). From Figure 8 it can be seen that the greatest amount of vertical displacement is along the Kunyere fault. Along the Thamalakane fault down throw is generally variable and changes along strike. As for the Phuti and Nare faults vertical displacement along them is very small (Fig 8). This therefore indicates that the Kunyere fault is the main westerly dipping bounding fault to the east of the rift system, consistent with its higher seismic activity (Reeves, 1972). The Kunyere and Thamalakane faults displace the dike swarm along its entire width, whereas the Phuti and Nare faults only displace the northern portion of the swarm (Fig.3 and 6). The southwestern extension of these latter faults intersects the southern portion of the dike swarm without any displacements. This therefore suggests that they may be pre-dike faults that have been partly reactivated in their northern section during Cenozoic rifting.

The Tsau and Lecha faults to the western part of the study area, show smaller depth to magnetic sources as compared to depth to magnetic sources along the Kunyere fault. Across the Tsau fault depth to magnetic sources generally decrease and this therefore suggest it is the main border fault to the west of the ORZ.

The faults mapped on the aeromagnetic maps except Lecha and Tsau have scarps associated with their surface expressions. The lack of surface expression for these basement faults (Lecha and Tsau faults) may suggest the following: inactivity during the extensional tectonic regime associated with the ORZ; that these basement faults were reactivated, but are now concealed by rapid sedimentation associated with Okavango alluvial fan deposits; they were reactivated but lacked sufficient energy to rupture (i.e., blind normal faults). The scarp heights of Kunyere Thamalakane and Phuti faults are significantly smaller than the fault throw values obtained from the 3-D Euler deconvolution solutions. This suggests either higher sedimentation rates from the Okavango River compared to the vertical movement along the faults leading to partial burial or moderate sedimentation rates against little to no vertical recurrent movement along the faults. Recent seismic events along the major rift faults support the higher sedimentation rates scenario (Scholz et al., 1976).

Within the ORZ, the major fault zones and their segments have orientations that parallel the structural fabric of the basement. This suggests that the strength anisotropy in the basement greatly influenced the location and orientation for brittle failure. The low displacement to length scaling relations observed for these faults may in part reflect a reduction in the stress

required to produce failure and laterally propagate faults along these pre-existing planes of weakness. In addition, comparison of the throw on the basement surface with the throw on the topographic fault scarp demonstrates many of the faults have extended histories. Most of the faults suggest evidence for multiple episodes of faulting with concomitant sedimentation along the down thrown block and erosion of the fault scarps (Kinabo et al., 2008).

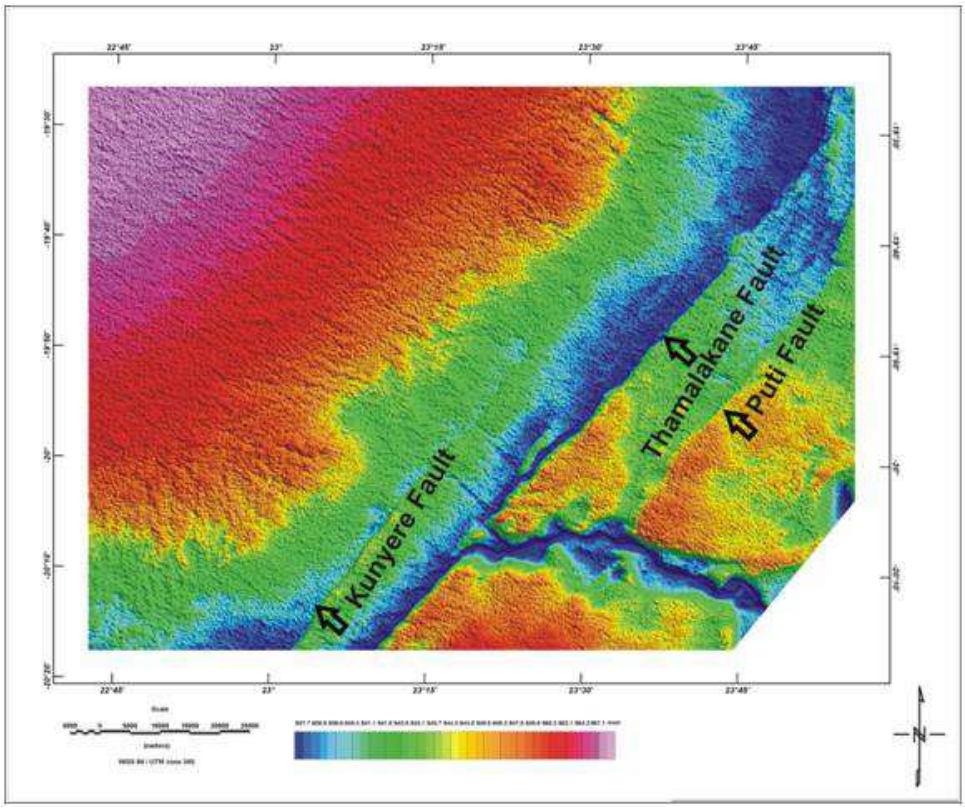

Fig. 5. Plot of SRTM_DEM for Eastern Margin of the ORZ (Study area)

Thus, older faults that have established long fault traces as a result of multiple episodes of faulting and through linking of fault segments may exhibit topographic scarps with less relief as a result of either the height of the topographic fault scarp reflecting only the most recent displacement event that ruptured the surface, or that since the last displacement, the height of the fault scarp has been reduced by sedimentation, or still the height of the fault scarp has been reduced by erosion.

Following the definition of Peacock and Sanderson, (1991), that border faults in rift zones have larger displacement and length and may indicate duplicity depending on the number of basin within the rift, it can be concluded that the border fault in the ORZ is still in the juvenile stage. This conclusion is solely based on the vertical displacements along faults obtained from 3-D Euler deconvolution solutions and length of the faults observed on the aeromagnetic data.

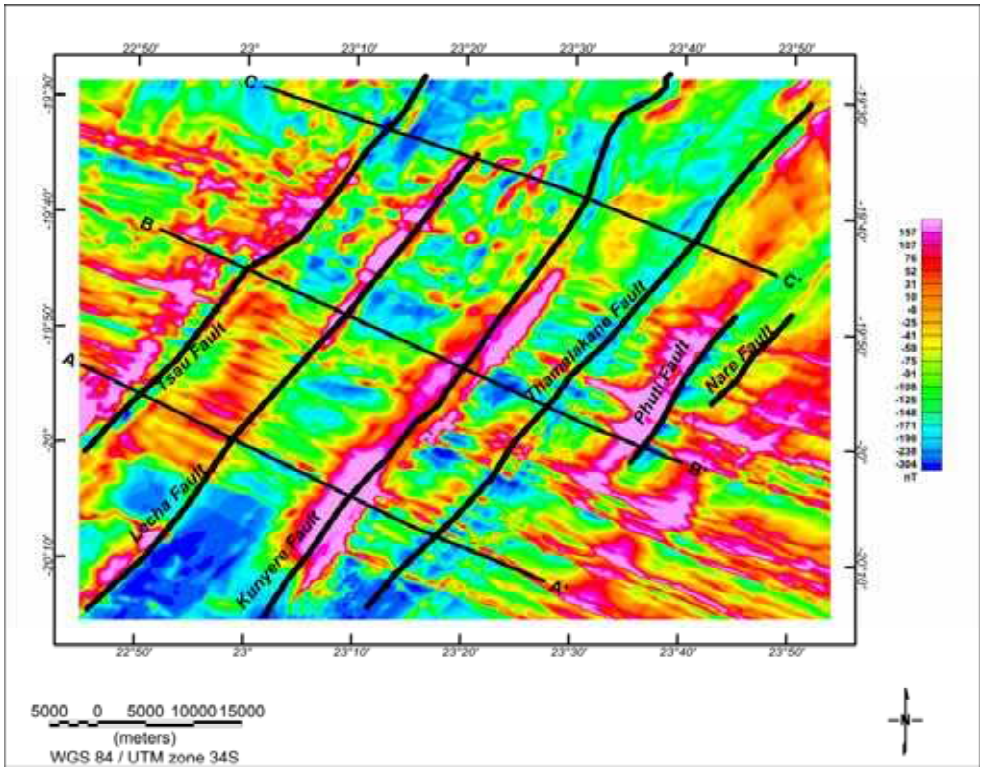

Fig. 6. Total magnetic field intensities over the study area (Note location of the 3 profiles selected across the Faults in the study area

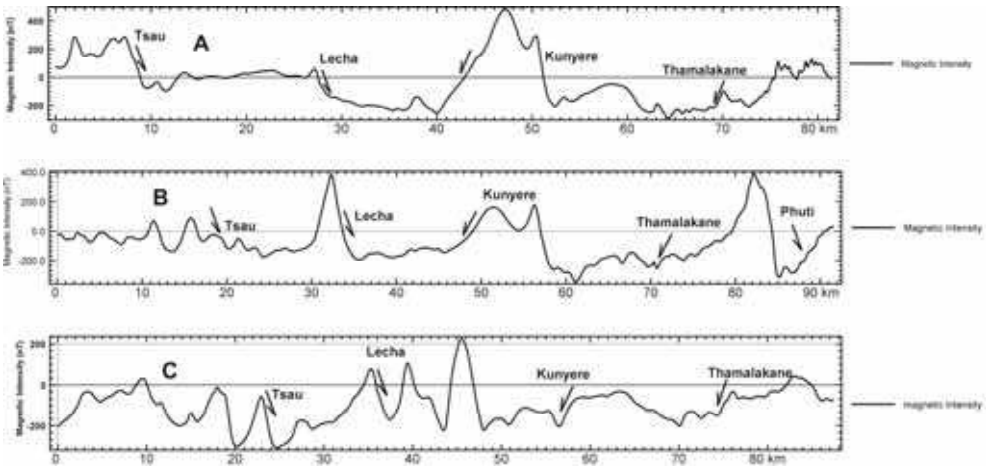

Fig. 7. Plot of the total magnetic field intensities along the 3 profiles selected across the Faults in the area (see Fig 6 for location of profiles)

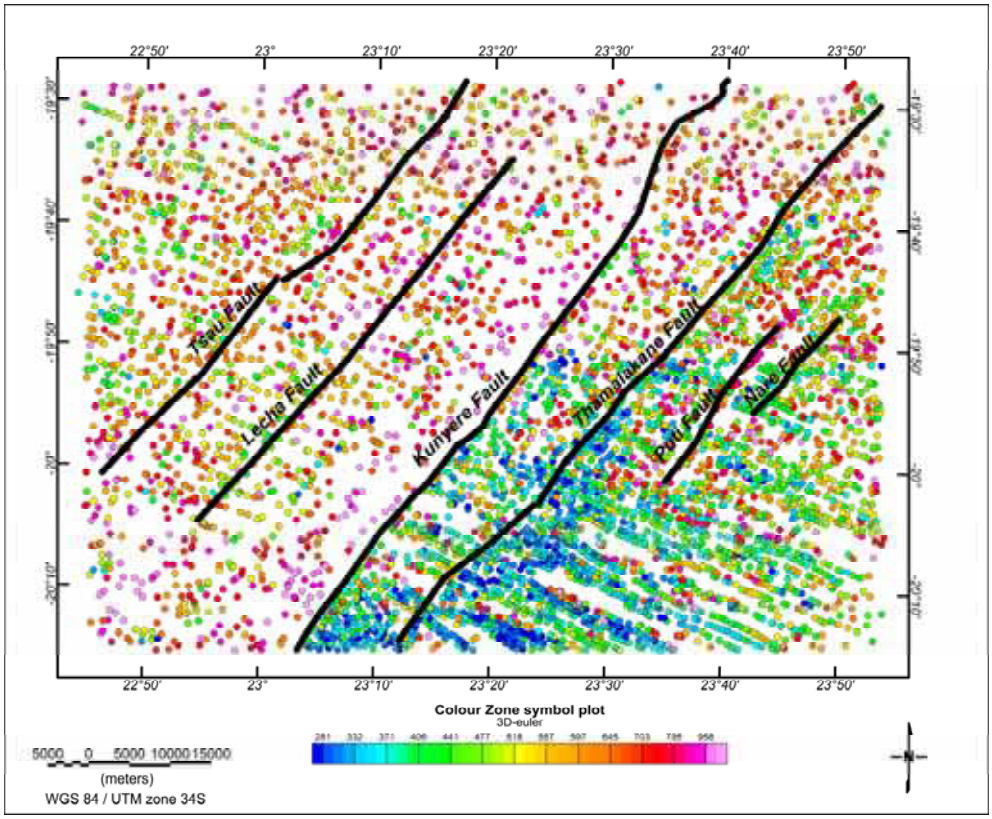

Fig. 8. Plot of Euler 3-D solutions obtained in the ORZ area

6.2 Rates of sedimentation and Fluvial Transfers and Seismicity in study area

According to McCarthy, (2005) and Gumbricht and McCarthy, (2003), the Okavango delta (part of the ORZ) receives enormous tonnage of bed load sediments and solute on yearly basis. McCarthy estimated that about 170,000 tonnes of sand and 360,000 tonnes of solute load enter the Okavango system every year. Bauer et al., (2006) also estimated that the Okavango delta receives about 870,000 tonnes of sediment per annum of which about 50% is made up of solutes, 22% is made up of particulate and 28% is made up of aeolian inputs. McCarthy (2005) estimated the average annual inflow into the Okavango to be 10.1 x 10^9 M^3 of water over the past 60 years. It is thought that these large amounts of water and solute load entering the ORZ on yearly basis plays a major role in the tectonic activities of the area The role of water and sediment load on seismicity in faulted zones has been investigated by previous researchers. An example of such a study is the geophysical studies of the San Andreas Fault (SAF) conducted by Unsworth et al., (1997); Mackie et al., (1998); Unsworth et al., (1999), Unsworth et al., (2000); Bedrosian et al., (2004); Unsworth & Bedrosian, (2004); and Ritter et al., (2005). Results of their studies suggested that seismic behavior may be controlled by a connected network of fluid-filled cracks within fault zones. Along the SAF, there is marked seismic variability, with some segments characterized by infrequent, large-

magnitude earthquakes while others exhibit abundant microseismicity and aseismic creep (Allen, 1968). These authors were able to establish a relationship between earthquakes and increase in fluid within the rock units. They also establish that fluid migration causes high pore pressure within rocks. The high pressure, in turn, ultimately reduces shear stress from the rock so that stress does not build to higher levels over time, which generates larger magnitude earthquakes.

Studies of seismic activities in the area of research indicate that seismicity increases substantially between the Kunyere Fault and the Thamalakane Fault, where it is thought that strain is being transferred from the Kunyere Fault to the Thamalakane Fault. Earthquakes in the study area are predominantly weak, except for the large earthquake events that were recorded during the May 1952 – May 1953 period, with magnitudes ranging between 5.0 and 6.7 on the Richter scale (Hutchins et al., 1976; Milzow et al., 2009). The Thamalakane Fault is believed to be channeling fluids in this area, as flow from the Okavango Delta is seen to disappear at this fault boundary. It is also thought that the northern segment of the Kunyere Fault may also be channeling fluids. Seismicity and fluid flow may have a direct relationship with faulting in the ORZ, similar to the SAF. A study performed by Brodsky and Kanamori (2001) suggests that lubrication by a viscous fluid within a fault zone can reduce the frictional stress during large earthquakes (M>4) by as much as 30%. The study suggested that any large earthquake that produces a slip distance of greater than a few meters along a fault plane during a single earthquake event will have a zone of the fault that is well lubricated. Lubrication of faults reduces high frequency energy due to contacting asperities during an earthquake. Consequently, large slip displacement and reduction in high frequency energy result in less damage. The fluids being channeled by the faults in the ORZ may allow for easier slip along the fault planes during large earthquakes.

The microseismicity and lack of high magnitude earthquakes associated with the northern segments between the Kunyere Fault and the Thamalakane Fault suggest that fluids within the fault zones and splays may raise pore pressure in this area of the rift thus reducing shear stress.

7. Conclusions

Six major northeast-trending faults have been mapped in the eastern margin of the ORZ; the Tsau, Lecha, Kunyere, Thamalakane, Phuti, and Nare faults. These faults displace the Karoo dykes and three of them (Kunyere, Thamalakane and Phuti) are represented by fault scarps. Depths to the top of the dikes show a deepening of the pre-Kalahari surface toward the northeastern part of the ORZ. The results of this study suggest that movement along the major Faults (Kunyere and Thamalakane) is dip-slip with the blocks downthrown to the west. The results of the study also suggest inflow of large amounts of fluids that are channeled along the major border faults on the eastern part of the ORZ (Kunyere and Thamalakane) may raise pore pressures in those area of the rift zone, thereby reducing shear stress. This phenomenon could account for the lack of large earthquakes and abrupt faulting within the ORZ.

8. Acknowledgment

The Department of Geological Surveys of the Ministry of Minerals, Energy and Water Resources of Botswana is greatly acknowledge for providing the aeromagnetic data used for the work.

9. References

Allen, C. (1968). The tectonic environments of seismically active and inactive areas along the San Andreas fault system. In: Dickinson, W. and Grantz, A. (eds) *Proceedings of Conference on Geologic Problems of the San Andreas Fault System,* pp. 70 - 82.

Bauer, P., Gumbricht, T. & Kinzelbach, W. (2006). A regional coupled surface water/ groundwater model of the Okvango Delta Botswana, *Water Resources Research.*, 42 W04403, doi:10.1029/ 2005WR004234.

Bedrosian, P.A., Unsworth, M.J, Egbert, G.D. & Thurber, C.H.(2004). Geophysical images of the creeping segment of the San Andreas fault: implications for the role of crustal fluids in the earthquake process: *Tectonophysics*, v. 385, pp. 137 - 158.

Briggs, I. C. (1974). Machine contouring using minimum curvature, *Geophysics*, 39, pp39-48.

Brodsky, E.E. & Kanamori, H.(2001). Elastohydrodynamic lubrication of faults: *Journal of Geophysical Research*, v. 106, No. 16, pp357 - 374.

Chen, L. & Lee, L. (1992). Progressive generation of control frameworks for image registration, *Photogrammetric Engineering and Remote Sensing*, No.58, pp. 1321-1328.

Cooke, H.J. (1984). The evidence from northern Botswana of climate change. In: Vogel, J (Eds.), *Late Cenozic palaeoclimates of the southern hemisphere*. Balkema, Rotterdam, pp. 265 - 278

Fairhead, J.D. & Girdler, R.W. (1969). How far does the rift system extend through Africa?: *Nature*, v. 221, p. 1018 - 1020.

Grauch, V. J. S. (2001). High-resolution aeromagnetic data, a new tool for mapping intrabasinal faults: Example from the Albuquerque basin, New Mexico. *Geology,* Vol. 29, No. 4, pp. 367–370.

Gumbricht, T. & McCarthy, T.S. (2003) Spatial Patterns of Island and Salt Crusts in the Okavango Delta, Botswana: *South African Geographical Journal*, v. 85, pp. 164 - 169.

Gumbricht, T., McCarthy, T.S., Merry, C.L. (2001). The topography of the Okavango Delta, Botswana, and its tectonic and sedimentological implications, *South African Journal of Geology*, 104:243-264

Hutchins, D.G., Hutton, S.M., Jones, C.R. & Loernhert, E.P. (1976). A summary of the geology, seismicity, geomorpholoygy and hydrogeology of the Okavango Delta: *Bulletin, Department of Geologic Surveys, Gaborone, Botswana.*

Kervyn, F., S. Ayub, Kajara, R., Kanza, E. & B. Temu, (2006). Evidence of recent faulting in the Rukwa rift (West Tanzania) based on radar interferometric DEM, *J African Earth Sci.*, vol. 44, pp. 151-169.

Kinabo B.D, Hogan, J.P, Atekwana, E.A, Abdelsalam, M.G, and Modisi, M.P (2008). Fault growth and propagation during incipient continental rifting: Insights from a combined aeromagnetic and Shuttle Radar Topography Mission digital elevation model investigation of the Okavango Rift Zone, northwest Botswana. *Tectonics* 27(3): TC3013, doi:10.1029/ 2007TC002154

Kinabo, B. D., Atekwana, E. A., Hogan, J. P., Modisi, M. P., Wheaton D. D. & Kampunzu, A. B. (2007). Early structural evolution of the Okavango Rift Zone, NW Botswana, *J African Earth Sci.,* vol. 48, pp 125-136.

Laletsang, K. (1995) Groundwater investigations using geophysical techniques at Marophe, the Okavango Delta, Botswana [M.S. thesis]: St. Johns, Memorial University of Newfoundland, 101 pp.

Mackie, R.L., Livelybrooks, D.W., Madden, T.R., and Larsen, J.C. (1997). A magnetotelluric investigation of the San Andreas fault at Carrizo Plain, California: *Geophysical Research Letters*, vol. 24, pp. 1847 - 1850.

McCarthy, T.S. (2005). Groundwater in the wetlands of the Okavango Delta, Botswana and its contribution to the structure and function of the ecosystem. *Journal of Hydrology*, Vol 320, pp. 264-282.

McCarthy, T.S., Smith, N.D., Ellery, W.N. & Gumbricht, T. (2001). The Okavango Delta - semiarid alluvial-fan sedimentation related to incipient rifting. In: Renaut, R.W., and Ashley, G.M. (eds), *Sedimentation in Continential Rifts, SEPM (Society for Sedimentary Geology) Special Publications*, vol. 70, pp. 179 - 193.

McCarthy, T.S., Stanistreet, I.G. & Cairncross, B., (1991). The sedimentary dynamics of active fluvial channels on the Okavango (Delta) alluvial fan, Botswana: *Sedimentology,* vol. 38, pp. 471 - 487.

Milzow, C., Kgotlhang, L., Bauer-Gottwein, P., Meier, P. & Kinzelbach W.,(2009), Regional review: the hydrology of the Okavango Delta, Botswana - processes, data and modelling: *Hydrogeology Journal*, vol. 17, pp. 1297 - 1328.

Modisi, M. P., Atekwana, E. A., Kampunzu, A. B. & T. H. Ngwisanyi, (2000). Rift Kinematics during the incipient stages of continental extension: Evidence from the nascent Okavango rift basin, northwest Botswana, *Geology*, vol. 28, pp. 939-942.

Modisi, M.P. (2000). Fault system of the southeastern boundary of the Okavango Rift, Botswana: *Journal of African Earth Sciences*, vol. 30, pp. 569–578.

Moore, A.E. & Larkin, P. (2001). Drainage evolution in south-central Africa since the breakup of Gondwana: *South African Journal of Geology*, vol. 104, pp. 47 - 68.

Peacock, D. C. P. & Sanderson, D. J. (1991), Displacements, segment linkage and relay ramps in fault zones, *J Struct. Geol. Vol.* 13, pp. 721-733.

Reeves, C.V. (1972). Rifting in the Kalahari?: *Nature,* vol. 237, pp. 95–96.

Ritter, O., Hoffmann-Rothe, A., Bedrosian, P.A., Weckmann, U. & Haak, V. (2005). Electrical conductivity images of active and fossil fault zones. From: Bruhn, D. and Burlini, L. (eds) 2005. High-Strain Zones: Structure and Physical Properties: *Geological Society of London, Special Publications*, vol. 245, pp. 165 - 186.

Scholz, C. H., Koczynski, T. A. & D. G. Hutchins, (1976). Evidence for incipient rifting in southern Africa. *Royal Astronomical Society Geophysical Journal,* vol. 44, pp. 135- 144.

Shaw, P. & Nash, D.J. (1998). Dual mechanisms for the formation of fluvial silcretes in the distal reaches of the Okavango Delta Fan, Botswana: *Earth Surface Processes and Landforms*, vol. 23, pp. 705 - 714.

Shaw, P. (1985). Late Quaternary Landforms and Environmental-Change in Northwest Botswana - the Evidence of Lake Ngami and the Mababe Depression: *Transactions of the Institute of British Geographers*, vol. 10, pp. 333 - 346.

Swain, C. J. (1976) A FOTRAN IV program for interpolating irregularly spaced data using the difference equations for minimum curvature, *Computer & Geosciences*, vol. 1, pp. 231-240.

Thomas, D.S.G. & Shaw, P.A. (1991). *The Kalahari Environment*:, Cambridge Univ., ISBN - 521-37080-9. New York 284 p.

Thompson, D.T. (1982). EULDPH - A technique for making computer-assisted depth estimates for magnetic data: *Geophysics*, vol. 47, pp. 31 - 37.

Unsworth, M. & Bedrosian, P.A. (2004). Electrical resistivity structure at the SAFOD site from magnetotelluric exploration: *Geophysical Research Letters*, vol. 31.Ll2SO3, d0i:lO.1029/ 2003GLOl9363

Unsworth, M.J, Bedrosian, P., Eisel, M., Egbert, G.D. & Siripunvaraporn, W. (2000). Along strike variations in the electrical structure of the San Andreas fault at Parkfield, California: *Geophysical Research Letters*, vol. 27, pp. 3021 - 3024.

Unsworth, M.J, Egbert, G.D. & Booker, J.R. (1999). High resolution electromagnetic imaging of the San Andreas fault in central California: *Journal of Geophysical Research*, vol. 104, pp. 1131 - 1150.

Unsworth, M.J, Malin, P.E., Egbert, G.D. & Booker, J.R. (1997). Internal structure of the San Andreas fault at Parkfield, California: *Geology*, vol. 25, pp. 359 - 362.

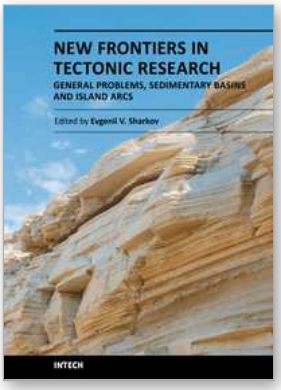

New Frontiers in Tectonic Research - General Problems, Sedimentary Basins and Island Arcs

Edited by Prof. Evgenii Sharkov

ISBN 978-953-307-595-2
Hard cover, 350 pages
Publisher InTech
Published online 27, July, 2011
Published in print edition July, 2011

This book is devoted to different aspects of tectonic research. Syntheses of recent and earlier works, combined with new results and interpretations, are presented in this book for diverse tectonic settings. Most of the chapters include up-to-date material of detailed geological investigations, often combined with geophysical data, which can help understand more clearly the essence of mechanisms of different tectonic processes. Some chapters are dedicated to general problems of tectonics. Another block of chapters is devoted to sedimentary basins and special attention in this book is given to tectonic processes on active plate margins.

INTECH
open science | open minds

InTech Europe
University Campus STeP Ri
Slavka Krautzeka 83/A
51000 Rijeka, Croatia
Phone: +385 (51) 770 447
Fax: +385 (51) 686 166
www.intechopen.com

InTech China
Unit 405, Office Block, Hotel Equatorial Shanghai
No.65, Yan An Road (West), Shanghai, 200040, China
中国上海市延安西路65号上海国际贵都大饭店办公楼405单元
Phone: +86-21-62489820
Fax: +86-21-62489821